INVESTIGATING OCEANUS PROCELLARUM BASALT FLOWS USING INTEGRATED CLEMENTINE UV-VIS AND NIR DATA. S. Z. Weider[1,2], I. A. Crawford[1] & K. H. Joy[1,2]. [1]Birkbeck/UCL Research School of Earth Sciences, Gower Street, London, WC1E 6BT, UK. [2]Space Science, Rutherford Appleton Laboratory, Didcot, Oxon, OX11 0QX, UK. (s.weider@ucl.ac.uk)

Introduction: The largest of the lunar maria, Oceanus Procellarum, is an area of particular interest in terms of choosing landing sites for future exploration of the Moon. It has been mapped previously by numerous authors [e.g. 1, 2] and been shown to consist of a large number of separate mare basalt flows, with estimated ages varying from 3.6 Ga to 1.2 Ga [1]. The study of geological samples collected from localities therein could provide important insights into a number of outstanding scientific issues. These include, further calibration of lunar crater chronologies [3], studying lunar mantle evolution through time [3], and the ancient history of the sun and inner solar system [4, 5].

This study: The aim of this work is to study an area within Oceanus Procellarum using both the UV-VIS [6] and the more recently calibrated NIR [7] Clementine datasets to further characterise the individual basalt flows and thereby understand better the geological history of the area.

The mineralogy and the FeO and TiO_2 wt. % compositions within fresh craters and their surrounding basalt flows (as mapped by [1]) are investigated. A search was also conducted for compositional differences between craters in the same flows, and possibly within craters themselves. Such differences would suggest that flows of discernibly different compositions were sampled during the crater forming events. Equations that provide quantitative estimates of the maximum excavation depth of the craters [8] can then be used to make estimates of the flow thicknesses, thus helping to constrain the total volumes of these lava flows.

An area (0° to 15°N; 45° to 60°W) in the equatorial region of Oceanus Procellarum was chosen because it is reported [1] to contain a particularly large number of different aged lava flows. Calibrated Clementine UV-VIS and NIR data for the area were downloaded at full resolution (~0.1 km/pixel) from the LPI [9] and USGS [10] websites respectively. Using codes written in IDL, these data were used to calculate FeO and TiO_2 wt. % abundances according to the algorithms of [11] and [12], and to construct 9-point reflectance spectra from nine of the eleven Clementine wavelength filters. Data were obtained at bandpasses centred around 415 nm, 750 nm, 900 nm, 950 nm, and 1000 nm (the UV-VIS bands) and at 1100 nm, 1250 nm, 1500 nm, and 2000 nm (the NIR bands).

By extracting data from different selected areas of craters (e.g. interior, rim, ejecta blanket), and their surrounding basalt flows, it is possible to characterise the composition and dominant mineralogies of the flows. Marked differences in these parameters between different areas of a crater (e.g. interior compared to ejecta blankets) are therefore suggestive of different flows being sampled vertically during the impact event and crater formation. If it is possible to match the characteristic composition of the average basalt flows to the differences in composition within a single crater, it should be possible to constrain the stratigraphy of the area and possibly the depth of the flows themselves. The diameter of the craters is measured using Lunar Orbiter photographs (i.e. Fig. 1) rather than Clementine images because they provide a much greater visual clarity.

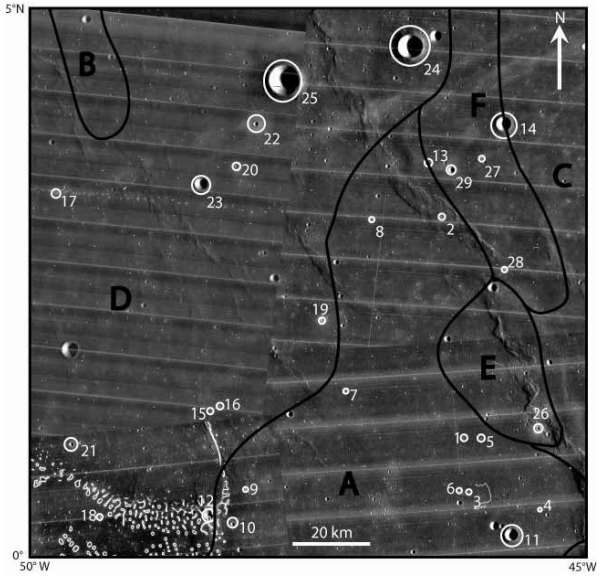

Figure 1. Area (45° to 50°W; 0° to 5°N) within equatorial Oceanus Procellarum showing basalt flow boundaries as mapped by [1] (marked by letters) on Lunar Orbiter images. Numbered are the 29 analysed craters.

Preliminary results: The area shown in Figure 1 is a small section of the total region that we are in the process of mapping. Basalt flows, as mapped by [1], are shown and labelled A – F, (corresponding to flows P67, P52, P47, P24 in [1]; additional flows are here labelled E and F, but were not named in the earlier study). Within this area, twenty-nine craters have been sampled and are identified numerically in Figure 1.

Basalt flows. A mean integrated UV-VIS and NIR reflectance spectrum (calculated from ten distinct inter-crater areas within the flow) for each of the basalt

flows is shown in Figure 2. In keeping with the methods of [11] this figure (also Fig. 3) shows the absolute reflectance values divided by a continuum line (defined as a straight line fitting the spectrum at 750 nm and 1500 nm) in order to enhance the absorption features. The depth of the absorption feature centred around 1 µm is controlled by the ferrous iron content of the soil as well as the amount of space weathering, therefore to obtain the FeO composition the two effects must be decoupled. The slope of the continuum line has been shown to correlate well with the amount of nanophase iron in lunar soils [11], therefore the continuum slope can be used to correct the 1 µm band depth for use in calculating the FeO wt.% composition. The dominant mafic mineralogy can be inferred from the NIR wavelength bandpasses because pyroxenes exhibit a second absorption band around 2 µm, but olivines do not. The relative abundances of these minerals can be deduced using a similarly space-weathering-corrected 2 µm band [11].

By characterising the flows in terms of their dominant mafic mineralogies as well as their FeO and TiO_2 wt.% compositions, a unique chemical signature for each can be identified. An integrated approach such as this, may highlight problems in the flows mapped in studies such as [1], or may help to corroborate their work. For instance, the flows A and F, which share a boundary, appear to be similar in both their spectral shape (Fig. 2) as well as their FeO and TiO_2 wt.% compositions, suggesting that perhaps the boundary does not actually exist.

Craters. Figure 3 shows the mean reflectance spectra from four different areas in and around crater 23 (diameter 3.7 km) within basalt flow D. The spectra are taken from a number of points: (i) within the crater itself (interior), (ii) the rim of the crater, (iii) the continuous ejecta blanket (assumed to extend for one crater radius beyond the crater itself, [13, 14]) and (iv) the surrounding basalt surface. These spectra, along with FeO and TiO_2 wt.% compositions from the same locations, can be used to map compositional differences within the crater. The maximum excavation depth of this simple crater is estimated to be ~300 m [8, 15].

From Figure 3 it is clear that underlying feldspathic highlands material has not been sampled (all spectra display the 1 µm absorption feature), therefore the total basalt thickness sampled by the crater must be >300 m, which is consistent with earlier studies [e.g. 16]. The calculated FeO wt % values are similar for each of the areas represented in Figure 3, therefore it would seem that the difference in spectra shapes seen here are due to varying levels of space weathering (consistent with findings from the methods of [12]). This is perhaps a little unexpected, because one would expect the interior, rim and ejecta levels of exposure to be similar, yet different from that of the surrounding basalt.

Conclusion: Studies such as that presented here, are important in developing our understanding of the compositional and mineralogical heterogeneity of mare basalts, and provide a new insight into the magmatic history of the Moon. By integrating the newly available Clementine NIR dataset with existing UV-VIS information it is possible to identify the dominant mineral phases of these deposits for the first time at a high spatial resolution.

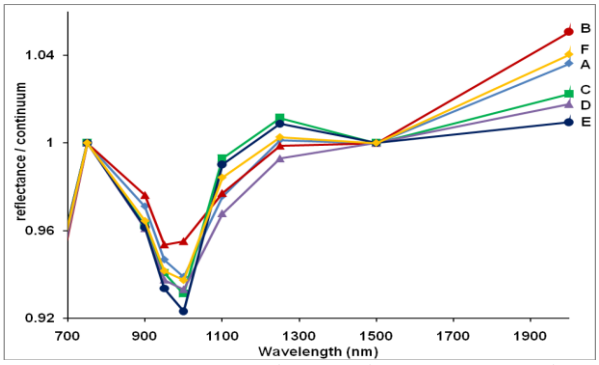

Figure 2. Mean spectral data for each of the mapped basalt flows (A-F) shown in Figure 1.

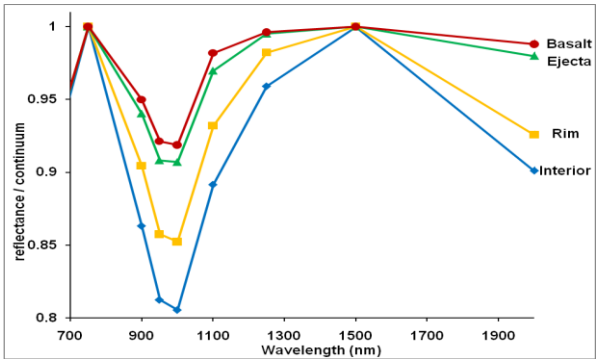

Figure 3. Reflectance spectra from different regions of crater 23 (diameter 3.7 km) within basalt flow D.

Acknowledgements: Thanks to Brian Fessler at the LPI for assistance writing the IDL codes used in this work. Thanks also to Barry Kellett for IDL assistance.

References: [1] Hiesinger, H. et al. (2003) *JGR, 108(E7),* 5065. [2] Pieters, C.M. (1978) *LPS IX,* 2825-2849. [3] Crawford, I. A. et al. (2007) *A&G, 48(3),* 18-21. [4] Spudis, P.D. (1996) The once and future moon, *Washington: Smithsonian Institution Press*. [5] Wieler, R. et al. (1996) *Nature, 384,* 46-49. [6] Eliason, E. et al. (1999) Mission to the Moon, The Clementine UVVIS Global Mosaic, PDS CL_4001-4078. [7] Gaddis, L. et al. (2007) The Clementine NIR Mosaic, PDS CL_5001-5078. [8] Stöffler, D. (2006) *Reviews in Mineralogy & Geochemistry, 60,* 519-596. [9] www.lpi.usra.edu/lunar/tools/clementine/ [10] www.mapaplanet.org [11] Le Mouélic, S. (2000) *JGR, 105(E4),* 9445-9455. [12] Lucey, P.G. et al. (2000) *JGR, 105(E8),* 20,297-20,305. [13] Moore, H.J. et al. (1974) *LPS V, 71-100.* [14] Oberbeck, V.R. et al. (1974) *LPS V, 111-136.* [15] Melosh, H.J. (1989) *Impact cratering a geologic process,* OUP. [16] Dehon, R.A. (1979) *LPS X,* 2935-2955.